

# Broadband absorption spectroscopy by combining frequency-domain and steady-state techniques

A. J. Berger<sup>1,2</sup>, F. Bevilacqua<sup>1</sup>, D. B. Jakubowski<sup>1</sup>, A. E. Cerussi<sup>1</sup>, J. Butler<sup>3</sup>, D. Hsiang<sup>3</sup>,  
B. J. Tromberg<sup>1</sup>

1. Laser Microbeam and Medical Program (LAMMP)  
Beckman Laser Institute, University of California, Irvine  
Irvine, CA 92612

2. The Institute of Optics, University of Rochester  
Rochester, NY 14627

3. Department of General Surgery, University of California,  
Irvine, CA 92697

## ABSTRACT

A technique for measuring broadband near-infrared absorption spectra of turbid media is presented using a combination of frequency-domain (FD) and steady-state (SS) reflectance methods. Most of the wavelength coverage is provided by a white-light SS measurement, while the FD data are acquired at a few selected wavelengths. Coefficients of absorption ( $\mu_a$ ) and reduced scattering ( $\mu_s'$ ) derived from the FD data are used to intensity-calibrate the SS measurements and to estimate  $\mu_s'$  at all wavelengths in the spectral window of interest. After these steps are performed,  $\mu_a$  can be determined by comparing the SS reflectance values to the predictions of diffusion theory, wavelength by wavelength. We present an application of this method to breast tumor characterization. A case study of a fibroadenoma is shown, where different absorption spectra were found between the normal and the tumor sides.

## 1. INTRODUCTION

We present a method using steady-state (SS) and frequency-domain (FD) reflectance measurements in tandem to obtain broad wavelength of the absorption coefficient spectra. This method is especially promising for tissue near-infrared spectroscopy, such as breast physiology characterization. For such applications, the method proposed here enables rapid data acquisition, deep tissue probing, and robust resolution of the contributions from the four major NIR tissue absorbers: oxy- and deoxy-hemoglobin, water, and fat. The central innovations are a) using FD-derived the absorption coefficient  $\mu_a$  and the reduced scattering coefficient  $\mu_s'$  values to convert the SS measurements into units of absolute reflectance, and b) using the power-law wavelength dependence of  $\mu_s'$  to obtain interpolated and extrapolated values at non-laser wavelengths. FD measurements are performed at a handful of diode laser wavelengths spanning the range of interest (650-1000 nm), while the SS measurements are performed continuously across the entire range. Unlike spatially-resolved SS, however, only a single, large source-detector separation is used, preferably the same one as for the FD measurements. The instrumentation is straightforward and particularly easy to add to an existing FD system.

In this paper, we first summarize the method (a complete description can be found in Ref.1), and second we present an application to breast tumor characterization.

## 2. MATERIALS AND METHOD

### 2.1. Optical measurements

Figure 1 shows the experimental arrangement for the combined SS and FD measurements. In all cases, light is delivered via optical fiber to the surface of the sample and collected at some distance away. The source detector separations were 21.5 (FD) and 24 (SS) mm (the slight difference was due to instrumental limitations; a future instrument will utilize identical distances). In FD mode (upper box), the light arrives sequentially from one of seven amplitude-modulated diode lasers (672, 800, 806, 852, 896, 913, and 978 nm, all with output powers of mW at the sample) and is detected by an avalanche photodiode unit (Hamamatsu C556P-56045-03) that amplifies the AC component of the signal. A network analyzer (Hewlett Packard 8753C) delivers 251 modulation frequencies between 100 and 700 MHz and measures phase and modulation amplitude of the photon intensity signal, as described elsewhere<sup>2</sup>. In SS mode (lower box), light comes from a 150W halogen lamp (Fiber-Lite) and is analyzed via a fiber-coupled spectrograph (Ocean Optics S2000) with a linear CCD detector between 525 and 1155 nm, with the useful range for our experiments being 650-1000 nm. The spectrograph records a total of 2048

points (0.35 nm/pixel), and the spectral resolution is 5 nm (full width at half maximum). Light is delivered to the sample using a bundle of four fibers (bundle diameter 600  $\mu\text{m}$ ) and collected using a single fiber of diameter 1 mm. The spectrum of the light source is measured separately by inserting the source and detector fibers into different ports of an integrating sphere (Labsphere, IS-040-SF). Relative reflectance is calculated to be the sample spectrum divided by the source spectrum (note

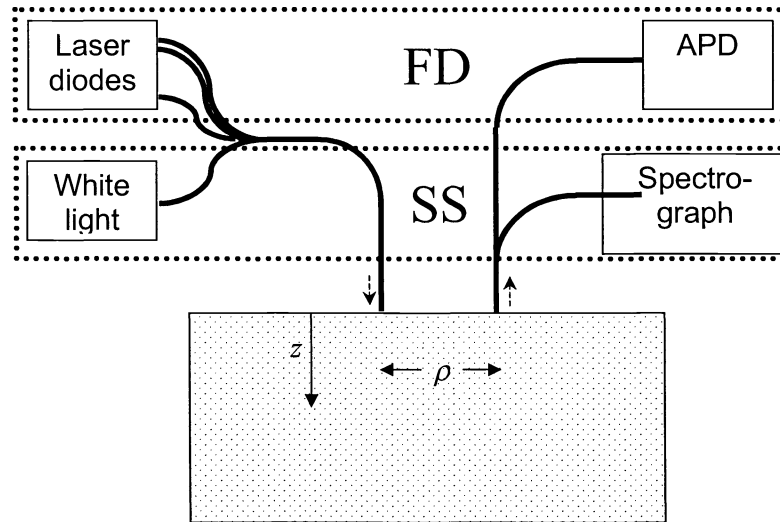


Figure 1. Configuration of light sources, optical fibers, and detectors: APD, avalanche photodiode. The dashed rectangles denote components that belong to the FD and SS systems.

that both measurements use the same delivery fiber, collection fiber, and detector apparatus). Total acquisition time per sample for SSFD measurements is on the order of 40 s (30 for FD and 10 for SS). Calculation of  $\mu_a(\lambda)$  was performed according to the methods of the next section using in-house Matlab (The MathWorks, Inc.) code, making use of the optimization toolbox.

## 2.2. Breast measurements

*In vivo* measurements were performed on the breasts of a supine female volunteer, age 37. Data were gathered from the left and right breasts. The right breast contained a fibroadenoma, which was located using a standard ultrasound imaging system. The tumor was approximately an ellipsoid of 10 and 20 mm of axial dimensions. The center of the tumor was approximately 12 mm deep.

For FD measurements, the source light was again delivered by optical fiber but the APD was placed directly against the tissue, without a collection fiber. Fiber and detector were bundled into a single handheld device that was placed gently against the breast. SS reflectance was measured subsequently, at the exact same location, in the two-fiber mode described above. All procedures were approved by the Institutional Review Board of the University of California, Irvine (study 95-563).

## 2.3. Method

The goal of these measurements is to obtain scattering parameters of the tissue and the concentration of Hb, HbO<sub>2</sub>, H<sub>2</sub>O and fat. Combining the information from the FD and SS measurements allows for the computation of the broadband absorption spectrum (650-1000 nm), which improved the accuracy of the determination of these chromophore concentrations (Hb, HbO<sub>2</sub>, H<sub>2</sub>O and fat). We summarize below the different steps of this calculation (see Ref.1 for a more complete description).

1. The frequency domain measurements are fit to a diffusion model<sup>3,4</sup>. The results of this fit provides the values of  $\mu_a$  and  $\mu_s'$  at the laser wavelengths (i.e. 672, 800, 806, 852, 896, 913, and 978 nm). For calibration, we gather FD data from a prepared sample whose  $\mu_a$  and  $\mu_s'$  values are known *a priori* from a set of two-distance frequency-domain measurements.
2. The  $\mu_a$  and  $\mu_s'$  values are used to predict the steady-state reflectance, using diffusion theory<sup>3,4</sup>. These reflectance values calculated for the lasers wavelengths are used to calibrate the steady-state reflectance  $R_{exp}(\lambda)$ . A simple linear fit allows us to

determine the calibration factor (independent of the wavelength, since the reflectance has been normalized first using an integrating sphere).

3. The discrete  $\mu_s'$  spectrum, obtained from the frequency domain measurements, is fit to a power function  $A\lambda^{-B}$  (see references 5,6 and 7). Using this fit,  $\mu_s'$  values are assigned for the entire spectrometer range (650-1000nm).

4. The  $\mu_a$  spectrum is calculated by solving numerically the equation

$$R_{exp}(\lambda) - R_{thy}(\mu_a(\lambda), \mu_s'(\lambda))=0.$$

In this equation,  $\mu_a(\lambda)$  is the only unknown since  $R_{exp}(\lambda)$  and  $\mu_s'(\lambda)$  are obtained from the procedures described on points 2 and 3, respectively.

### 3. RESULTS AND DISCUSSION

We present here two measurements illustrating the potential of the method for tumor characterization. The first measurement was performed on the top of a fibroadenoma, and a control measurement was performed on the other breast (symmetrically at the same location).

Fig 2. shows the calibrated reflectance spectrum (line), along with the reflectance data calculated from the frequency domain measurements (diamonds). This figure illustrates the fact that, as expected, a single scaling factor is sufficient to fit well the measured steady-state reflectance and the predicted reflectance from frequency domain measurement.

It can be noted that significant differences between the normal and tumor sides are already found at this stage of analysis. Nevertheless, to interpret these differences from a physiological point of view, we need to transform these spectra into absorption spectra. Indeed, the access to the absorption spectrum allows us to determine physiologically relevant parameters such as the concentrations of  $H_b$ ,  $H_bO_2$ ,  $H_2O$  and fat.

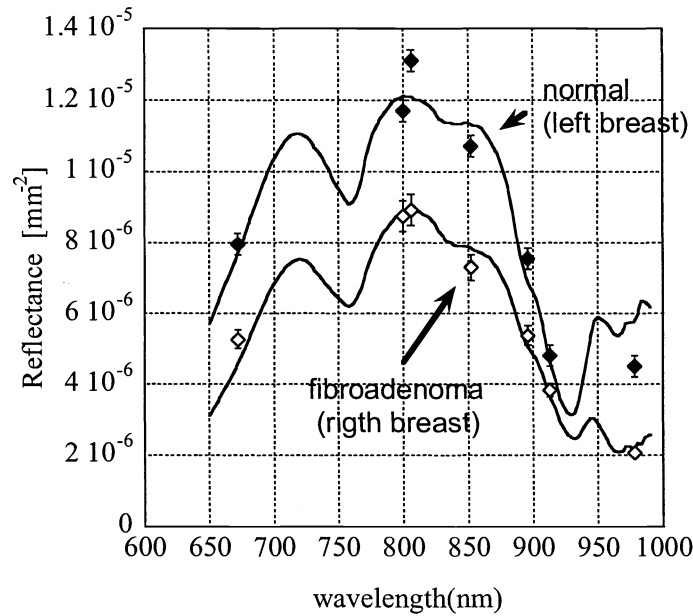


**Figure 2.** Measured reflectance spectra (line) and calculated reflectance from frequency domain data (diamonds). The measured reflectance spectra are scaled to fit the calculated reflectance points.

The determination of the absorption spectrum requires the knowledge of the reduced scattering parameters  $\mu_s'$  at all wavelengths. These values are obtained from a fit of the  $\mu_s'$  values derived from frequency domain measurements to a power function (Figure 3). In this particular case, no significant differences in the scattering properties were found between the normal and tumor sides. Nevertheless, such a finding should not be generalized, since usually differences are also naturally found between normal and tumor tissues.

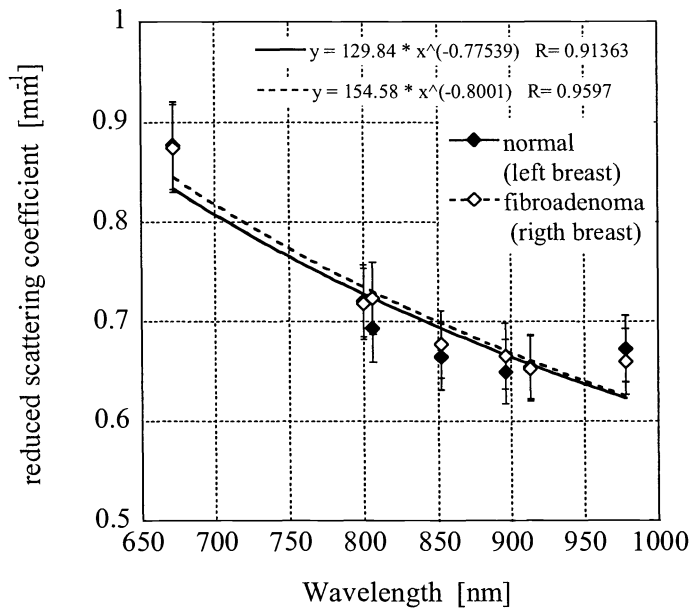


**Figure 3.** Interpolation of reduced scattering coefficient from frequency domain data (diamonds). The reduced scattering values are fitted to a power function  $A\lambda^{-B}$  (lines).

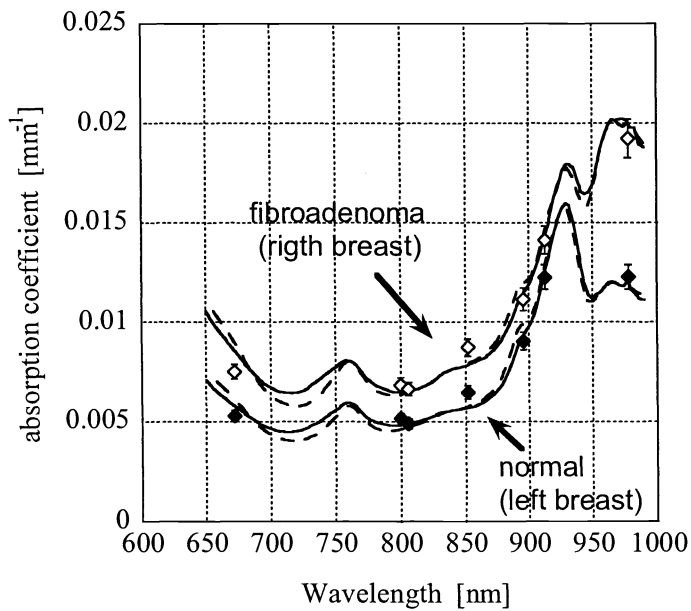


**Figure 4.** Computed absorption spectra (line) and reflectance from frequency domain data (diamonds). The absorption spectra are linearly fitted to the  $\text{Hb}$ ,  $\text{HbO}_2$ ,  $\text{H}_2\text{O}$  and fat absorption spectra (broken line). The concentrations values are reported in Table 1.

**Table 1.** Chromophore concentrations. The concentration of H<sub>2</sub>O and fat are related to pure H<sub>2</sub>O and 100% soybean oil.

	total Hb (mM)	O <sub>2</sub> saturation (%)	water (%)	fat (%)
Left breast normal	0.0216	70.4	13.3	74.0
Right breast: fibroadenoma	0.0354	74.0	19.3	80.8

The information contained in Figures 2 and 3 are finally used to derive the absorption spectra, shown in Figure 4.

As expected the differences found in the reflectance spectra (Fig.2) are again found here. Note the very good agreement between the absorption coefficient values from frequency domain and the computed continuous spectra (Fig4). Figure 4 shows clearly that more information is contained in the continuous spectra compared to the frequency domain only points. Various chromophores can be easily identified by their peaks; such as the H<sub>b</sub> peak at 760 nm, the fat peak at 930 nm and the H<sub>2</sub>O peak at 975 nm. These absorption spectra can be approximated by the linear combination of the four chromophores mentioned earlier H<sub>b</sub>, H<sub>b</sub>O<sub>2</sub>, H<sub>2</sub>O and fat (absorption spectra from references 8, 9 and 10 respectively). The results of these fits are shown in Figure 4 (broken line), and the concentrations are reported in Table 1. The quality of these fits is good, which confirms that these chromophores are the predominant ones in breast tissues.

The main differences between the normal and tumor sides are found in the total hemoglobin concentration (64% higher in the tumor side) and in the water concentration (45% higher in the tumor). The increase of hemoglobin concentration is due to the denser vascularization, as generally found in tumors. The increased water concentration is probably due to necrosis and edema. The concentrations found here as well as the differences between normal and tumor tissue are consistent with earlier findings<sup>11,12</sup>.

#### 4. CONCLUSION

A combination of SS and FD reflectance measurements has been described for absorption spectroscopy of turbid media, featuring beneficial aspects of both techniques. As with SS, the wavelength coverage is continuous, detecting absorption features that may elude the discrete wavelengths chosen for FD. The prediction of constituent concentrations, for instance in breast tissue, is substantially improved using full-spectrum absorption data rather than a handful of wavelengths. As with FD, however, only a single source-detector separation is required, making the technique more amenable to reporting volume-averaged values for heterogeneous samples. In addition, the source-detector separation can be large, allowing for centimeter-scale mean probing depths that cannot be achieved with spatially-resolved SS techniques. An application to breast analysis has been demonstrated, with quantitative *in vivo* spectra of human breast obtained rapidly (less than 1 min.). Significantly different spectra were found between normal and fibroadenoma tissues. The technique is relatively inexpensive and could prove valuable for improving accuracy in the development of quantitative photon migration for clinical instruments.

#### 5. ACKNOWLEDGMENTS

This work was supported by the National Institutes of Health (NIH) under grant Nos. GM50958 and RR01192 (Laser Microbeam and Medical Program: LAMMP), the Department of Energy (DOE No. DE-FG03-91ER61227), and the Office of Naval Research (ONR No. N00014-91-C-0134). The authors gratefully acknowledge postdoctoral fellowships from the George E. Hewitt Foundation for Medical Research (AJB), the Swiss National Science Foundation (FB), and US Army grant DAMD17-98-1-8186 (AEC). Facilities and support of the Avon breast center in the Chao Family Comprehensive Cancer Center at UC Irvine were utilized to complete clinical portions of this study.

#### REFERENCES

1. F. Bevilacqua, A. J. Berger, A. E. Cerussi, D. Jakubowski, and B. J. Tromberg, "Broadband absorption spectroscopy in turbid media by combined frequency-domain, main and steady-state methods", *Appl. Opt.* **39**, 6498-6507 (2000).
2. T. H. Pham, O. Coquoz, J. B. Fishkin, E. Anderson, and B. J. Tromberg, "Broad bandwidth frequency domain instrument for quantitative tissue optical spectroscopy," *Rev. Sci. Instr.* **71**, 2500-2513 (2000).
3. R. C. Haskell, L. O. Svaasand, T.-T. Tsay, T.-C. Feng, M. S. McAdams, and B. J. Tromberg, "Boundary conditions for the diffusion equation in radiative transfer," *J. Opt. Soc. Am.* **11**, 2727-2741 (1994).
4. A. Kienle and M. S. Patterson, "Improved solutions of the steady-state and the time-resolved diffusion equations for reflectance from a semi-infinite medium," *J. Opt. Soc. Am.* **14**, 246-254 (1997).

5. R. Graaff, J. G. Aarnoose, J. R. Zijp, P. M. A. Slood, F. F. M. de Mul, J. Greve, and M. H. Koelink, "Reduced light-scattering properties for mixtures of spherical particles: a simple approximation derived from Mie calculations," *Appl. Opt.* **31**, 1370-1376 (1992).
6. J. R. Mourant, T. Fuselier, J. Boyer, T. Johnson, and I. J. Bigio, "Predictions and measurements of scattering and absorption over broad wavelength ranges in tissue phantoms," *Appl. Opt.* **36**, 949-957 (1997).
7. J. M. Schmitt and G. Kumar, "Optical scattering properties of soft tissue: a discrete particle model," *Appl. Opt.* **37**, 2788-2797 (1998).
8. S. Wray, M. Cope, D. T. Delpy, J. S. Wyatt, and E. O. R. Reynolds, "Characterization of the near-infrared absorption spectra of cytochrome-AA3 and hemoglobin for the non-invasive monitoring of cerebral oxygenation," *Biochim. et Biophys. Acta* **933**, 184-192 (1988).
9. L. H. Kou, D. Labrie, and P. Chylek, "Refractive indexes of water and ice in the 0.65  $\mu\text{m}$  to 2.5  $\mu\text{m}$  spectral range," *Appl. Opt.* **32**, 3531-3540 (1993).
10. C. Eker, Ph.D. thesis, Lund University, 1999, *Optical characterization of tissue for medical diagnostics*.
11. M. J. Holboke, B. J. Tromberg, X. LI, N. Shah, J. Fishkin, D. Kidney, J. Butler, B. Chance, and A. G. Yodh, "Three-dimensional diffuse optical mammography with ultrasound localization in a human subject", *J. Biomed. Opt.* **5**, 237-247, 2000.
12. R. Cubeddu, A. Pifferi, P. Taroni, A. Torricelli, and G. Valentini, "Noninvasive absorption and scattering spectroscopy of bulk diffusive media: An application to the optical characterization of human breast," *Apl. Phys. Lett.* **74**, 874-876 (1999).